Masthead combiner employing asynchronously coupled resonant junctions

Ogbodo, E. A.; Wu, Y.; Callaghan, P.; Wang, Y.

DOI:
10.23919/EuMC.2018.8541754

Document Version
Peer reviewed version

Citation for published version (Harvard):
Ogbodo, EA, Wu, Y, Callaghan, P & Wang, Y 2018, Masthead combiner employing asynchronously coupled resonant junctions. in *2018 48th European Microwave Conference (EuMC).* Institute of Electrical and Electronics Engineers (IEEE), pp. 695-698. https://doi.org/10.23919/EuMC.2018.8541754

Masthead Combiner Employing Asynchronously Coupled Resonant Junctions

Eugene A. Ogbodo*, Yun Wu, Peter Callaghan, and Yi Wang

Department of Engineering Science, University of Greenwich
Kent, ME4 4TB, United Kingdom
*eugene.ogbodo@gmail.com

***Abstract*— This paper proposes the use of asynchronously coupled resonator junctions in the design of a masthead combiner (MHC). By employing the resonator junctions, a miniaturised circuit is achieved without using any transmission-line based impedance matching circuits. The main challenge in the design is the control and implementation of the external couplings at the common ports of this all-resonator-based MHC. A four-port microstrip MHC operating at the two channels of 1.8 and 2.1 GHz has been demonstrated with a fractional bandwidth of 1.764 GHz to 1.836 GHz and 2.058 GHz to 2.142 GHz respectively. Good agreements have been achieved between the measurements of the prototype devices and the simulations.**

I. Introduction

In many communication systems, the transceiver is connected to an antenna using a selective diplexer which permits the transmitter (TX) and receiver (RX) to share a common antenna [1-3]. The antenna is mostly mounted on the top of a communication mast, so transmission lines with a considerable length will be required for the transceiver connection, which introduces additional losses and worsens the overall noise figure of the receiving system. This scenario is illustrated in Fig. 1.

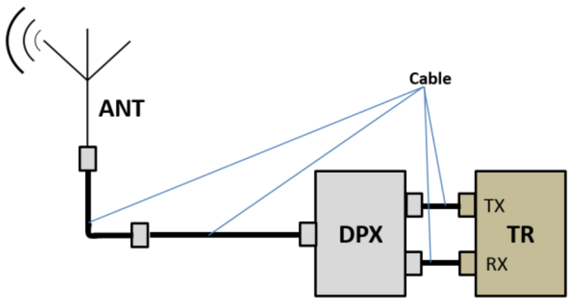

Fig. 1 Connection in a traditional antenna and transceiver module

The degradation of noise figure caused by the cable losses could be compensated by introducing a Low Noise Amplifier (LNA) at the receiver chain while preserving the connection of TX to the antenna [4-5]. A MastHead Combiner (MHC) is such a device that allows the addition of the LNA as illustrated in Fig. 2. It is a passive device with four ports. It is made up of three filters. The RX_1 and RX_2 filters of the MHC provides the protection and filtering for the LNA from the TX signal. RX_1 and RX_2 work at the same frequency. It is worth mentioning that these filters (RX_1, RX_2 and TX) may possess multi-band response depending on the application requirement [5].

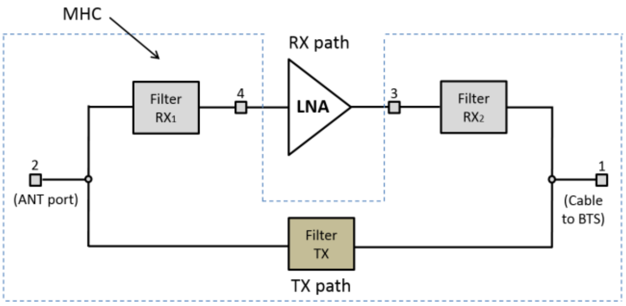

Fig. 2 Masthead combiner allowing the introduction of an LNA to the RX chain

There are very few works on MHC reported in the open literature and majority of them are waveguide based. This paper presents a novel implementation using microstrip technology and is built on from the design concept of resonant junctions [6-10] and multi-port filtering networks [11]. Asynchronously coupled resonator junctions, previously demonstrated in [11-12], are used to ease the control and implementation of the external couplings at the common port 1 and 2 (Fig. 2).

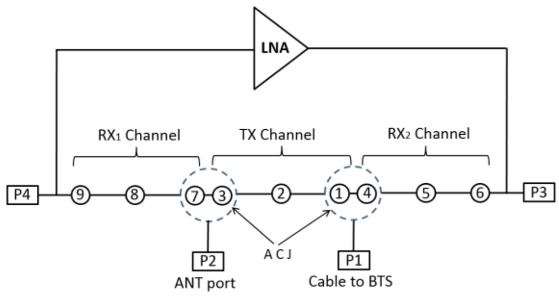

Fig. 3 Coupling topology of the proposed masthead combiner with an LNA connected.

II. Masthead Combiner Design

A. *Layouts of MHC*

Fig. 3 presents the coupling topology of the proposed MHC with a block diagram of an LNA (not included in the design). Two asynchronously coupled junctions (ACJ), resonators 3-

and-7 and resonators 1-and-4, are used. The resonators 1, 2 and 3 represent the TX filter while the resonators 7, 8 and 9 represent the RX_1 filter and resonators 4, 5 and 6 represent the RX_2 filter. This makes the MHC more like a double diplexer sharing one TX filter in one branch. RX_1 and RX_2 operate at 2.1 GHz and TX at 1.8 GHz. All three channel filters have a three-pole Chebyshev ripple factor of 0.043 dB, a 4% fractional bandwidth (FBW) and a 20 dB return loss. Hairpin resonators were used for the design of the filters. The circuit layout is presented in Fig. 4 with the optimised dimensions.

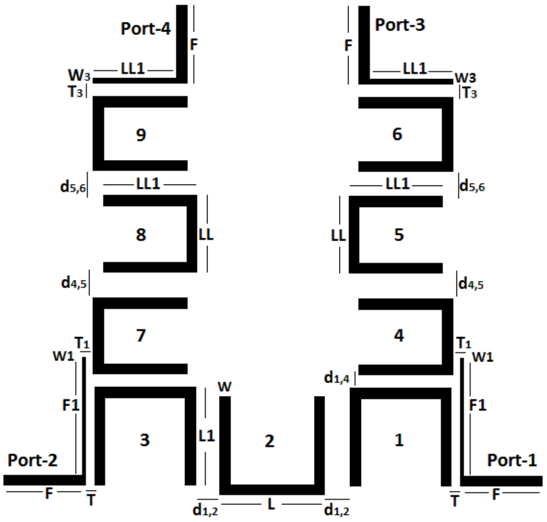

Fig. 4 Layout of the microstrip MHC: F = 10mm, T = 0.4mm, T1 = 0.2mm, T3 = 0.4mm, W = 1.2mm, W1 = 0.4mm, W3 = 0.6mm, L = 9.85mm, L1 = 11.5mm, LL = 6.6mm, LL1 = 11mm, d1,2 = 1.7mm, d1,4 = 0.2mm, d4,5 = 1.6mm, d5,6 = 1.6mm

To form the proposed MHC, the three channel filters were first separately designed to specifications. These filters are designed to meet the three-pole Chebyshev ripple factor of 0.043 dB with a lowpass prototype derived from [13-14] with g-values of g0 = g4 = 1.0, g1 = g3 = 0.8516, and g2 = 1.1032. The g-values are used in obtaining the coupling coefficients and external Q-factors used for the physical dimensioning of the resonators. Using the general filter synthesis method, the coupling coefficients and external quality factors were derived from (1) and (2) [14-15].

$$M_{1,2} = M_{2,3} = M_{4,5} = M_{5,6} = \frac{FBW}{\sqrt{g_1 g_2}} = 0.041 \tag{1}$$

$$Q_{ex1(L)} = Q_{ex1(H)} = Q_{ex2} = Q_{ex3} = \frac{g_1 g_0}{FBW} = 21.29 \tag{2}$$

where $Q_{ex1(L)}$ and $Q_{ex1(H)}$ are the external Q-factors from the common port to the low and high channel respectively.

B. *Asynchronous Coupling and Q_{ext}*

To join the channel filters to form the MHC, the ACJ structure was used. To achieve the ACJ, the first resonators of the TX and RX_2 channels, that is resonator 1 and 4, were asynchronously coupled together to define the two channel frequencies as shown in Fig. 5.

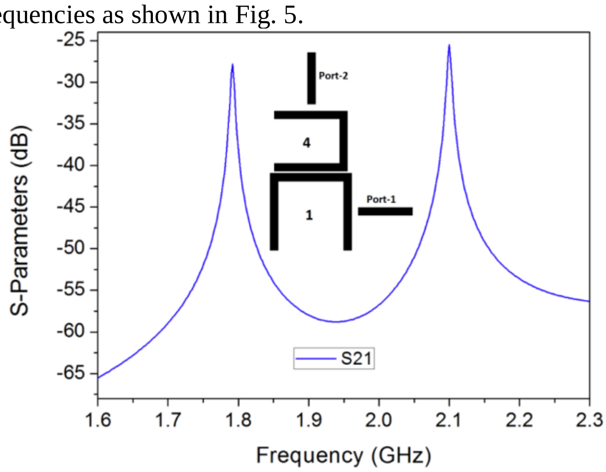

Fig. 5. Asynchronous coupling between resonator 1 and 4.

To achieve the external quality factors (Q_{ext}) from the common port to the ACJ, a coupled feed line was used as shown in Fig. 6. Port-2 and port-3 in Fig. 6 were weakly coupled to the resonators whereas the coupling gap, width and length of the feed line were adjusted to achieve the required Q_{ext} using (3).

$$Q_{ex1(L)/(H)} = \frac{f_{1(L)/(H)}}{\Delta f_{1(L)/(H)}} \tag{3}$$

where $f_{1(L)/(H)}$ and $\Delta f_{1(L)/(H)}$ are the centre frequencies and the 3 dB bandwidths of the resonance curves corresponding to the low and high channel. Fig. 6 presents a graph of the design curve. Due to symmetry, the ACJ containing resonators 3 and 7 is the same as the ACJ with resonators 1 and 4.

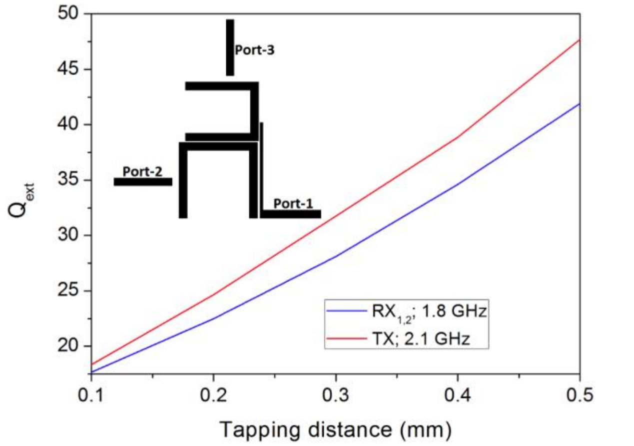

Fig. 6. Design curve of the responses of the configuration used to extract Q_{ext}

III. Results

The EM software Sonnet is used for the simulation. Fig. 7 presents the simulated responses of the MHC for the RX_1 filter and the TX filter. Due to symmetry, the frequency response of the RX_2 filter and the TX filter will be identical to that of the RX_1 and TX filter. The responses achieved in the simulation met the specification of 4% FBW and 20 dB return loss at both passbands with an isolation around 30 dB. The current distribution of the MHC at the TX and RX_1 channels are presented in Fig. 8.

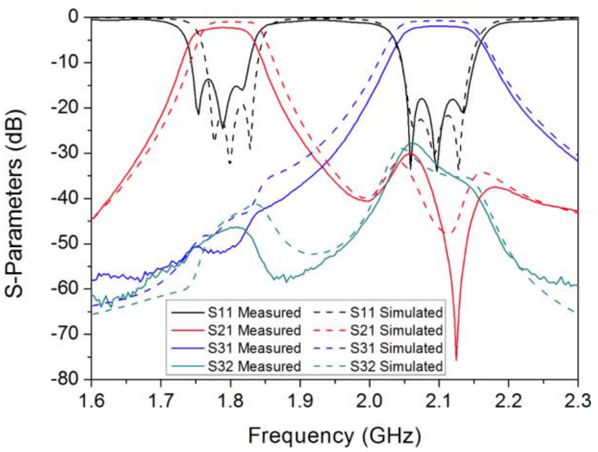

Fig. 7 Simulated response in comparison with the measured.

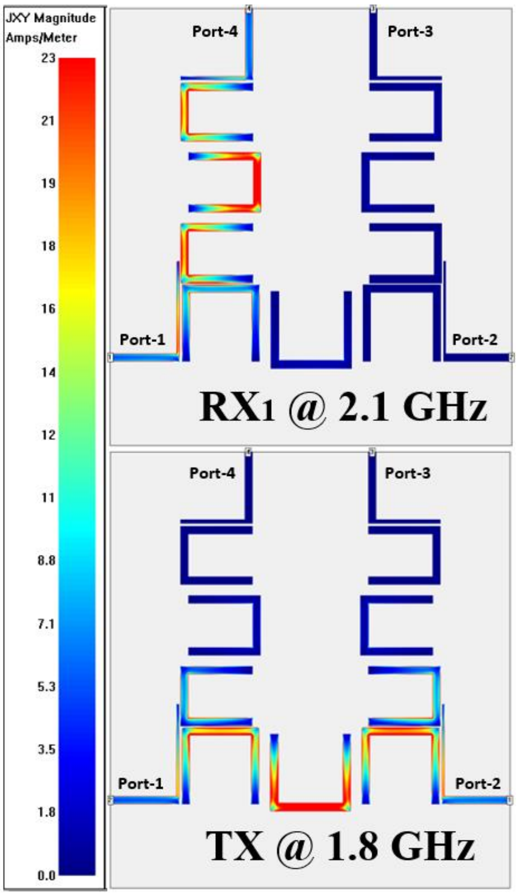

Fig. 8 Simulated current density distribution at the TX and RX1 channels

Rogers 3010 substrates with a thickness of 1.27mm, a relative permittivity of 10.8 and a loss tangent of 0.002 were used for prototyping. The prototyped design is presented in Fig. 9. Measurements were taken using Agilent Network Analyser N5230A. Fig. 7 compares the simulated responses of the proposed MHC (dash lines) with the measured responses (solid lines). Reasonably good agreement between the simulated and measured responses has been achieved. The measured TX channel has a frequency shift of about 10 MHz to the left and a bandwidth of 5 MHz more than the simulated response. The return loss is 15 dB with an insertion loss of 2.5 dB. The measured RX_1 and RX_2 channels have approximately the same bandwidth with the simulated response. A return loss of 18 dB and insertion loss of 2 dB were recorded. The measured isolation is higher than 28 dB at the RX_1 and RX_2 channel and 48 dB at the TX channel.

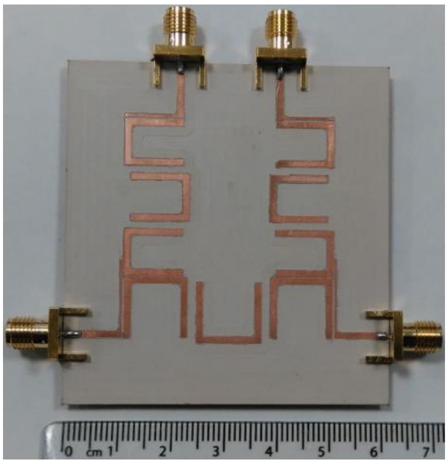
Fig. 9 Prototyped MHC circuit

IV. Conclusions

In this work, asynchronously coupled resonant junctions are used in the design of resonator-based MHC using the multi-port filtering networks technique. The design demonstrated the feasibility of realising a MHC by controlling the external coupling to the resonator junction. It represents a new implementation technique for masthead combiners using a compact coupling topology.

References

[1] E. A. Ogbodo, Y. Wu and Y. Wang, "Microstrip diplexers with dual-mode patch resonant junctions," 2016 46th European Microwave Conference (EuMC), London, United Kingdom, 2016, pp. 1155-1158.

[2] Y. Wu, Y. Wang and E. A. Ogbodo, "Microstrip wideband diplexer with narrow guard band based on all-resonator structures," 2016 46th European Microwave Conference (EuMC), London, United Kingdom, 2016, pp. 1163-1166.

[3] T. Yang, P. L. Chi and T. Itoh, "High Isolation and Compact Diplexer Using the Hybrid Resonators," in IEEE Microwave and Wireless Components Letters, vol. 20, no. 10, pp. 551-553, Oct. 2010.

[4] S. Tamiazzo, G. Macchiarella "Design and realization of filtering units in a triple-band masthead amplifier system for BTS of mobile communications", IEEE MTT-S Int. Microwave Symp. Dig., Seattle, Jun. 2013

[5] G. Macchiarella and S. Tamiazzo, "Design of "masthead" combiners," 2015 European Microwave Conference (EuMC), Paris, 2015, pp. 686-689.

[6] X. Guan, W. Huang, H. Liu, P. Wen, Q. Chen, A. Ouyang, Y. Liu, "A novel microstrip diplexer with a common square ring resonator for

WCDMA," 2016 IEEE International Workshop on Electromagnetics: Applications and Student Innovation Competition (iWEM), Nanjing, 2016, pp. 1-3.
[7] K. L. Wu and W. Meng, "A Direct Synthesis Approach for Microwave Filters With a Complex Load and Its Application to Direct Diplexer Design," in IEEE Transactions on Microwave Theory and Techniques, vol. 55, no. 5, pp. 1010-1017, May 2007.
[8] X. Shang, Y. Wang, W. Xia and M. J. Lancaster, "Novel Multiplexer Topologies Based on All-Resonator Structures," in IEEE Transactions on Microwave Theory and Techniques, vol. 61, no. 11, pp. 3838-3845, Nov. 2013.
[9] M. F. Hagag, M. Abu Khater, M. D. Hickle and D. Peroulis, "Tunable SIW Cavity-Based Dual-Mode Diplexers With Various Single-Ended and Balanced Ports," IEEE Transactions on Microwave Theory and Techniques, vol. PP, no. 99, pp. 1-11.
[10] P. Zhao and K. L. Wu, "Model-Based Vector-Fitting Method for Circuit Model Extraction of Coupled-Resonator Diplexers," IEEE Transactions on Microwave Theory and Techniques, vol. 64, no. 6, pp. 1787-1797, June 2016.
[11] E. A. Ogbodo, Y. Wu, P. Callaghan, and Y. Wang, "Asynchronous Coupling Resonant Junctions for Compact Diplexers and Multi-Port Filtering Networks," Microwave and Optical Technology Letters, 2017.
[12] E. A. Ogbodo, Y. Wu, P. Callaghan, and Y. Wang, "A Compact Diplexer with a Split-Ring Resonator Junction," Microwave and Optical Technology Letters, 2017.
[13] J.-S. Hong "Microstrip Filters for RF/Microwave Applications," John Wiley & Sons, Inc. 2011.
[14] D. M. Pozar, Microwave Engineering. 3rd ed. New York: Wiley, 2005.
[15] J. Y. Lin, S. W. Wong, L. Zhu, Y. Yang, X. Zhu and Y. He, "A Dual-Functional Triple-Mode Cavity Resonator with the Integration of Filters and Antennas," IEEE Transactions on Antennas and Propagation, vol. PP, no. 99, pp. 1-1, Feb. 2018.
[16] E. A. Alós, A. U. Zaman and P. S. Kildal, "Ka-Band Gap Waveguide Coupled-Resonator Filter for Radio Link Diplexer Application," IEEE Transactions on Components, Packaging and Manufacturing Technology, vol. 3, no. 5, pp. 870-879, May 2013.